Mosquitoes integrate visual and acoustic cues to mediate conspecific interactions in swarms

Current biology : CB

Gupta, Saumya; Cribellier, Antoine; Poda, Serge B.; Roux, Olivier; Muijres, Florian T. et al

https://doi.org/10.1016/j.cub.2024.07.043

Article

Current Biology

Mosquitoes integrate visual and acoustic cues to mediate conspecific interactions in swarms

Graphical abstract

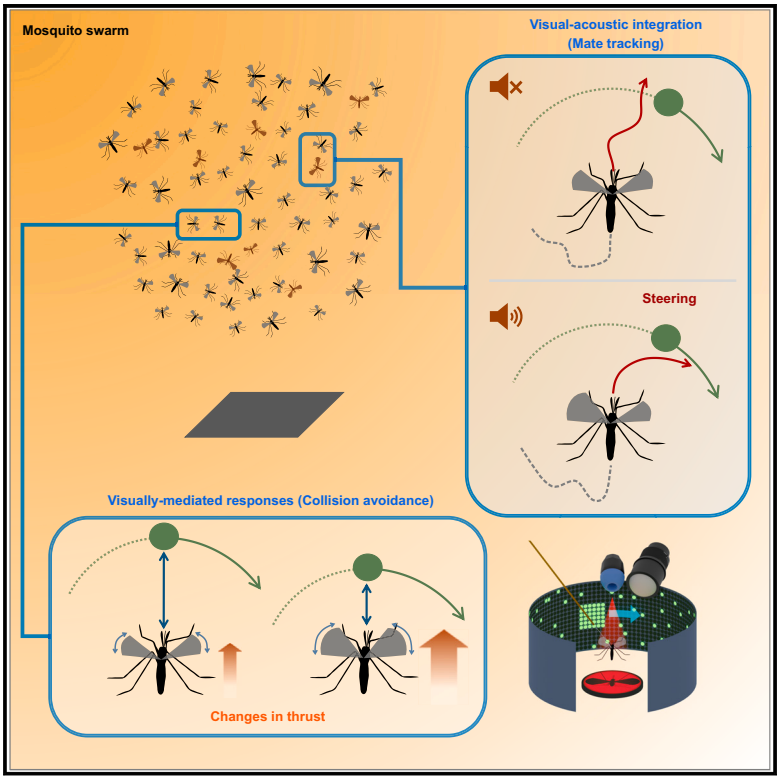

Authors

Saumya Gupta, Antoine Cribellier, Serge B. Poda, Olivier Roux, Florian T. Muijres, Jeffrey A. Riffell

Correspondence

jriffell@uw.edu

In brief

Swarming mosquitoes must navigate their complex environments to locate mates. Gupta et al. study how they use sensory cues to perform this task. They find that while mosquitoes respond to visual cues mimicking nearby conspecifics, hearing the flight tone of a potential mate changes their visual response by triggering attraction toward these cues.

Highlights

- The flight tone of a potential mate modulates visual responses in mosquitoes
- Males steer toward nearby visual objects in the presence of a female flight tone
- Visual cues alone modulate wing kinematics that contribute to thrust production
- Thrust-based forces are also modified in free-flight collision-avoidance scenarios

Gupta et al., 2024, Current Biology *34*, 4091–4103
September 23, 2024
https://doi.org/10.1016/j.cub.2024.07.043

CellPress

Current Biology

CellPress

Article

Mosquitoes integrate visual and acoustic cues to mediate conspecific interactions in swarms

Saumya Gupta,[1] Antoine Cribellier,[2] Serge B. Poda,[2,3] Olivier Roux,[3,4] Florian T. Muijres,[2] and Jeffrey A. Riffell[1,5,6,7,*]
[1]Department of Biology, University of Washington, Seattle, WA 98195, USA
[2]Experimental Zoology Group, Wageningen University, De Elst 1, 6708 WD Wageningen, the Netherlands
[3]Institut de Recherche en Sciences de la Santé (IRSS), 01 BP 2779, Bobo-Dioulasso, Burkina Faso
[4]MIVEGEC, University of Montpellier, IRD, CNRS, 34394 Montpellier, France
[5]X (formerly Twitter): @RiffellLab
[6]Bluesky: @riffelllab.bsky.social
[7]Lead contact
*Correspondence: jriffell@uw.edu
https://doi.org/10.1016/j.cub.2024.07.043

SUMMARY

Male mosquitoes form aerial aggregations, known as swarms, to attract females and maximize their chances of finding a mate. Within these swarms, individuals must be able to recognize potential mates and navigate the social environment to successfully intercept a mating partner. Prior research has almost exclusively focused on the role of acoustic cues in mediating the male mosquito's ability to recognize and pursue females. However, the role of other sensory modalities in this behavior has not been explored. Moreover, how males avoid collisions with one another in the swarm while pursuing females remains poorly understood. In this study, we combined free-flight and tethered-flight simulator experiments to demonstrate that swarming *Anopheles coluzzii* mosquitoes integrate visual and acoustic information to track conspecifics and avoid collisions. Our tethered experiments revealed that acoustic stimuli gated mosquito steering responses to visual objects simulating nearby mosquitoes, especially in males that exhibited a strong response toward visual objects in the presence of female flight tones. Additionally, we observed that visual cues alone could trigger changes in mosquitoes' wingbeat amplitude and frequency. These findings were corroborated by our free-flight experiments, which revealed that *Anopheles coluzzii* modulate their thrust-based flight responses to nearby conspecifics in a similar manner to tethered animals, potentially allowing for collision avoidance within swarms. Together, these results demonstrate that both males and females integrate multiple sensory inputs to mediate swarming behavior, and for males, the change in flight kinematics in response to multimodal cues might allow them to simultaneously track females while avoiding collisions.

INTRODUCTION

Lekking is a remarkable behavioral strategy documented across various species in which individuals congregate at specific areas—termed leks—to engage in competitive displays with the ultimate aim of securing a mate.[1,2] This strategy, widely studied in birds and mammals, is also paralleled in the insect world, where swarms formed for the purpose of mating function as analogous structures to leks.[3] However, unlike the static gatherings seen in many lekking species, flying insects such as dance flies, mayflies, midges, and mosquitoes form highly dynamic mating swarms.[4–6] In these swarms, individuals navigate through a complex three-dimensional space, introducing the challenges of aerial maneuvering to an already complicated in-flight mating ritual. Successful mating within these swarms thus hinges on the ability of individuals to avoid collisions in the complex sensory environment while pursuing mates.[7] *Anopheles* mosquitoes, known for their role in the transmission of malaria-causing pathogens, are one group of swarm-forming insects whose mating success holds significant consequences for public health.[8,9] Yet, the sensorimotor mechanisms that regulate avoidance and attraction among conspecifics within these swarms remain largely unknown.

The swarming behavior of the *Anopheles gambiae s.l.* mosquitoes, representing the best characterized mating behavior among mosquitoes,[10–12] serves as an excellent model for understanding the sensorimotor mechanisms operating within swarms. As dusk falls, mosquitoes of this species complex begin to aggregate over visual landmarks, forming swarms that serve as mating arenas. These swarms are predominantly composed of males, who compete for the relatively few females in the swarms. Males actively pursue females for copulation while managing to avoid collisions with other males, presumably by maintaining a specific inter-individual distance.[7] Such spatial navigation within swarms suggests an advanced sensory mechanism at play, one that is critical yet not fully understood. Several studies have revealed that males rely on their acute ability to detect the distinct flight tones of females, which are produced at a different frequency than their own, to identify and pursue potential mates.[13–16] On the contrary, males are much less

sensitive to the flight tones of other males and may not always be able to acoustically detect one another.[17–21] This selective acoustic sensitivity suggests the potential existence of other sensory mechanisms beyond auditory processing that facilitate individual detection and collision avoidance within swarms.

Previous research has established that mosquitoes can integrate multiple sensory inputs, including visual, thermal, and olfactory cues.[22–25] For example, host-associated olfactory cues can trigger mosquitoes to initiate visual search behaviors, even in nocturnal ones like *Anopheles*.[24,26] This capability to simultaneously process and integrate multiple sensory cues is believed to be crucial for host-seeking activities and is likely instrumental in other behavioral contexts, including swarming. Within swarms, where buzzing mosquitoes—up to thousands in case of *Anopheles*—occupy a fixed volume, the resulting sensory landscape rich in acoustic and visual information suggests that mosquitoes may also use their visual system for detecting fellow swarming individuals.[27] Whether mosquitoes employ their visual system along with their auditory system to interact with conspecifics within the dynamic setting of swarms remains to be tested.

In this study, we tested the hypothesis that *Anopheles* mosquitoes utilize visual cues of flying individuals in conjunction with acoustic information from their wingbeats to approach potential mates and avoid collisions with conspecifics. This hypothesis challenges the widely held belief that *Anopheles* mosquitoes rely minimally on visual cues for detecting other individuals due to their poor visual acuity, estimated at an angular resolution of 16.7°.[28] However, it is important to recognize that flying insects, despite their low spatial resolution, are generally well-adapted to visually detect moving targets representing prey, predator, or mates.[29]

We investigated our visual-acoustic integration hypothesis using a combined tethered-flight and free-flight experimental approach. In our tethered experiments, we used a virtual reality flight simulator to examine the behavioral response of rigidly tethered *Anopheles coluzzii* to moving objects in the presence or absence of conspecific sounds. In our free-flight experiments, we examined free-flight responses of *Anopheles coluzzii* in swarms and compared these with responses in the tethered state. Our work, leveraging these approaches, reveals the importance of sensory integration in shaping conspecific interactions within mosquito mating swarms.

RESULTS

Anopheles mosquitoes respond to swarm-like visual scenes

Our initial experiment assessed whether *Anopheles* mosquitoes could detect visual characteristics of swarms, such as the presence of small, sparsely distributed objects. We simulated such a visual environment on a two-dimensional cylindrical LED panel by displaying random starfield patterns with 10% of the LEDs illuminated. This setup aimed to reflect the density of contrasting elements visible against the backdrop of the sky, as observed in the natural swarm imagery (Figure 1A).

To evaluate whether mosquitoes could detect these simulated swarm-like scenes, we presented both male and female mosquitoes with static starfield patterns and monitored their behavioral response as the pattern drifted horizontally, in clockwise or counterclockwise (yaw) directions. This moving starfield was designed to elicit a widefield motion perception, typically inducing an optomotor response. In tethered flying insects, this response results in steering behavior, characterized by differential wingbeat amplitudes of the left and the right wings (L − R WBAs), directing the insects toward the motion.[30–32]

Our analyses revealed that both male and female mosquitoes exhibited an optomotor response to the visual stimuli (Figure 1B, top row). Compared to their baseline response when the starfield pattern was static, both sexes exhibited a significant steering toward the direction of the moving pattern (Figure 1C, top row; males: $p = 0.035$, $t = 2.16$, $df = 51$; females: $p = 0.025$, $t = 2.31$, $df = 48$, paired t test). Responses were similar for both clockwise and counterclockwise motion after accounting for the direction (males: $p = 0.73$, $\beta = 0.17$, SE = 0.50, $df = 26$; females: $p = 0.14$, $\beta = -0.96$, SE = 0.63, $df = 25$, linear mixed-effect model), supporting averaging the responses to both stimulus motion directions for comprehensive analysis.

These optomotor responses were also coupled with changes in aerodynamic thrust production,[33] as evidenced by increased total WBA (Figures 1B and 1C, middle row; males: $p = 0.004$, $t = 3.03$, $df = 51$; females: $p < 0.001$, $t = 4.23$, $df = 48$) and wingbeat frequency (WBF) (Figures 1B and 1C, bottom row; males: $p = 0.014$, $t = 2.56$, $df = 51$; females: $p < 0.001$, $t = 5.09$, $df = 48$).

Comparative analysis showed no significant differences in steering and thrust responses between males and females (L − R WBA: $p = 0.396$, $t = -0.85$, $df = 79.61$; L + R WBA: $p = 0.075$, $t = -1.80$, $df = 85.26$; WBF: $p = 0.874$, $t = 0.16$, $df = 72.02$, Welch two sample t test).

These results collectively highlight the potential of *Anopheles* to detect aspects of the visual environment of natural swarms and may suggest that the observed optomotor responses could stabilize an individual within a drifting swarm of conspecifics.

Acoustic cues modulate visual object tracking

Next, we investigated whether visual cues could play a role in shaping conspecific interactions, particularly in the contexts of mate attraction and collision avoidance. Based on our hypothesis that *Anopheles* mosquitoes combine visual and acoustic information, we predicted that mosquitoes would exhibit acoustically dependent visual responses. Specifically, we expected that without a conspecific flight tone present, mosquitoes would steer away from visual objects, indicative of collision avoidance. In contrast, if the same object is accompanied by the flight tone of a potential mate, the mosquitoes would steer toward the visual objects. Given mosquitoes' antennae and sensory neurons are not tuned to detect the flight tones of same-sex individuals,[13,34,35] we expected that mosquitoes would steer away from visual objects paired with same-sex flight tones.

To test these predictions, we simulated the visual cue of a nearby flying mosquito within a swarm on our LED panel by displaying a square object with a 22.5° optical angle, moving against a dark starfield background (Figure 2A). This optical angle approximates the angular size of a mosquito viewed by another mosquito from a distance of 2.4 body lengths. We monitored the steering responses of individuals as the object moved horizontally (yaw) from one side to the other. To further add the biological context of whether the visual object represents a male or a female mosquito, we designed additional stimulus

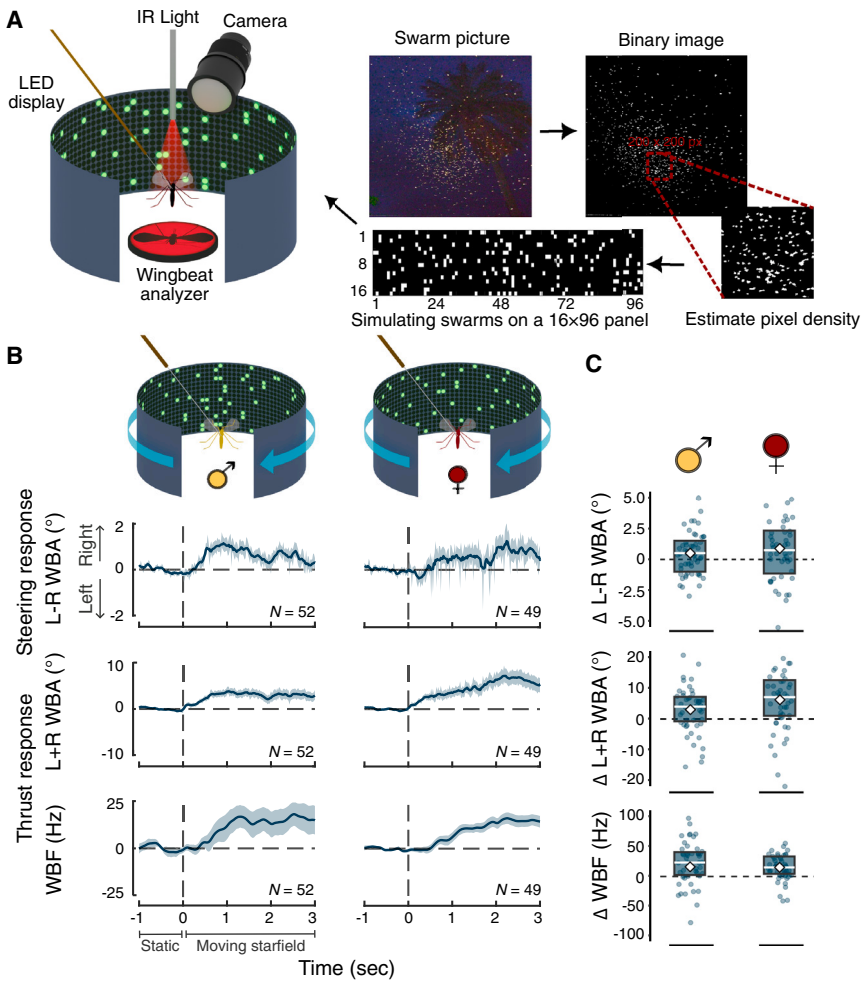

Figure 1. *Anopheles* mosquitoes behaviorally respond to simulated swarm-like visual scenes

(A) Illustration of the visual flight simulator, which includes an LED panel for presenting visual stimuli and a camera and wingbeat analyzer to record wing kinematics of tethered mosquitoes. The panel displays starfield pattern derived from binarized images of actual *Anopheles* swarms. Each pixel subtends an angle of 3.75° on the mosquito eye, which stimulates a mosquito that is ~15 body lengths away. The pattern aims to replicate the contrast density of mosquitoes observed in natural swarms against the background of the sky.

(B) Mean normalized behavioral responses of male (left) and female (right) *An. coluzzii* to visual stimuli. Shaded regions represent the standard error (± SE). Top panel shows steering responses measured by difference in left and right wingbeat amplitude, while the middle and bottom panels display additional thrust response measured by total wingbeat amplitude and wingbeat frequency, respectively. The data are averaged across both clockwise and counterclockwise motion and standardized for clockwise rotation.

(C) Statistical analysis of male (left) and female (right) responses, shown via boxplots, quantifies the change in response from the 1 s of pre-stimulus baseline (static) to the last 1 s of the stimulus presentation (moving starfield). Boxplot elements include the interquartile range (box boundaries), mean (diamond), and median (horizontal line), with individual data points that fall within at least 95% quantile range. White symbols and lines for mean and median denote statistical significance ($p < 0.05$). In this experiment, all measured responses during stimulus presentation significantly differed from baseline.

presentations in which the moving object was concurrently broadcast with species-specific flight tones (female-like flight tone at 450 Hz and male-like flight tone at 700 Hz) (Figure 2A).

In supplemental experiments, we showed that similar to free-flying males,[36,37] tethered males exhibited steering responses toward the direction of the female flight tone (Figure S1). Therefore, in this set of experiments, we fixed the position of the speaker in front of the tethered mosquito to ensure that all responses were due to visual stimuli. This experimental design also resulted in our decision to use a rigidly tethered setup over a magnotether system,[38,39] which would have allowed for free rotation of mosquitoes around the yaw axis but would have altered the relative orientation of the head to the sound source.

Contrary to our initial expectations and in contrast to their responses to the starfield (widefield) motion, mosquitoes did not exhibit steering toward or away from the moving object when presented alone. Analysis of their steering behavior showed no significant deviations from baseline for either males ($p = 0.648$, $t = -0.46$, $df = 45$; paired t test) or females ($p = 0.387$, $t = -0.87$, $df = 45$ $p = 0.387$, $t = -0.87$, $df = 45$) in the absence of acoustic cues (Figures 2B, top row, and 2C).

However, in the presence of female tones, males exhibited a strong response toward the object by significantly steering in the direction of the object's motion (Figures 2B, middle left column, and 2C; $p = 0.011$, $t = 2.66$, $df = 46$). The average steering response was highly correlated with the object's position (r = 0.77), and the mean response at the object's zero crossing (the object was directly in front of the mosquito) was significantly above zero ($p < 0.01$, $t = 3.72$, $df = 46$, t test), suggesting phase-advanced steering behavior that is seemingly predictive or anticipatory.[40] In contrast, the presence of male tones did not elicit steering toward or away from the moving object (Figures 2B, bottom left column, and 2C; $p = 0.718$, $t = 0.36$, $df = 44$). However, a moderately positive correlation was observed between the males' steering behavior and the object's position during male tone presentation (r = 0.68), which suggests that males slightly altered their steering behavior in response to the object's location.

For females, the presence of female flight tones did not alter their steering response (Figures 2B, middle right column, and 2C; $p = 0.973$, $t = 0.03$, $df = 43$). However, in the presence of male tones, although females did not exhibit significant steering toward the object (Figures 2B, bottom right column, and 2C; $p = 0.957$, $t = -0.05$, $df = 44$), their steering responses were highly correlated with the position of the moving object (r = 0.83; also refer to Figure S2) with the mean steering response at zero crossing being close to zero ($p = 0.730$, $t = 0.35$, $df = 44$). This suggests that females tracked the visual object in the presence of a mate's tone, aligning their steering closely with the object's location.

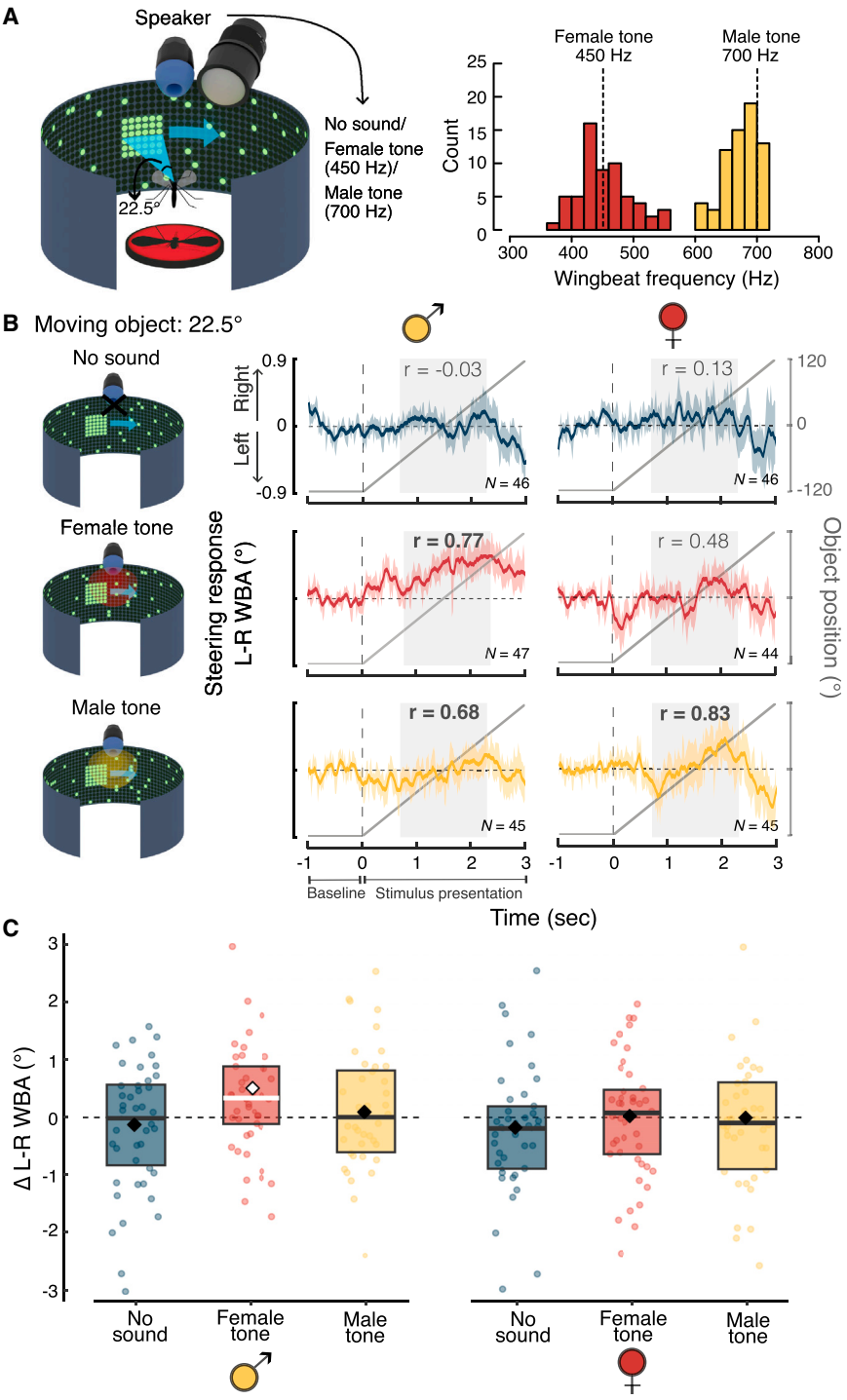

Figure 2. Acoustic modulation of object tracking in males and females

(A) Illustration of the tethered-flight setup used in this experiment. A square object against a starfield pattern, subtending at angle of 22.5° at the mosquito's eye, simulates a visual cue of a nearby mosquito within a swarm. An earphone, fixed in front of the tethered mosquito (see Figure S1), delivers either a female-like tone at 450 Hz or a male-like tone at 700 Hz (these values are based on previous literature[35] and the distribution of tethered female [red] and male [yellow] wingbeat frequencies recorded when mosquitoes were not presented with any visual or acoustic cue).

(B) Mean normalized steering responses of tethered male (left) and female (right) *An. coluzzii* to the 22.5° square object during a pre-stimulus baseline condition when the object was static (−1 to 0 s) and during the stimulus presentation when object moved horizontally (0–3 s), with or without accompanying acoustic cues. Responses are averaged for over both directions of object motion and standardized to represent motion from left to right. Shaded regions represent standard error (± SE). The solid gray line indicates the location of object, with 0° representing it directly in front of the mosquito. r value on each plot indicates Spearman's correlation between average steering response and the object position during the time segment highlighted by light gray shaded region. Values highlighted in bold signify moderate to strong correlation (r > 0.6). The full dynamics of steering responses before, during, and after stimulus presentation can be seen in Figures S2 and S3.

(C) Statistical analysis of male (left) and female (right) responses, shown via boxplots, quantifies the change in response from a pre-stimulus baseline to stimulus presentation. Boxplot elements include the interquartile range (box boundaries), mean (diamond), and median (horizontal line), with individual data points that fall within at least 95% quantile range. Mean and median symbols and lines are color coded with white denoting statistical significance ($p < 0.05$).

These results reveal that *Anopheles* mosquitoes integrate visual and acoustic information and highlight a potentially important role of visual cues in shaping behavioral dynamics during conspecific interactions.

Acoustic modulation of visual object tracking depends on object size

Building on our findings that acoustic cues can trigger *Anopheles* mosquitoes, especially males, to track a visual object, we further investigated whether these responses varied with object size. Given that the perceived size of a mosquito changes with distance, understanding this relationship is crucial in the natural context. Therefore, we presented male mosquitoes with square objects of 37.5°, 22.5°, and 15°, which represent the size of mosquitoes at distance of 1.3, 2.4, and 3.7 body lengths, respectively. These angular sizes were selected to align with the visual resolution capabilities of this species and fall within a range that is relevant for inter-individual interactions within swarms.

We observed that responses to the 37.5° object were similar to responses to the previously tested 22.5° object: in the absence of acoustic cues, males did not significantly steer in response to the visual cue (Figure 3A, top columns 1 and 2; $p = 0.512$, $t = -0.68$, $df = 45$). However, with the addition of female flight

tones, they exhibited a steering response in the direction of the object's motion (Figures 3A, middle columns 1 and 2, and 3B; $p = 0.026$, $t = 2.3$, $df = 44$), with their mean steering response at zero crossing again being significantly above than zero ($p = 0.049$, $t = 2.03$, $df = 44$). The male flight tones did not elicit a similar steering behavior in males as female tones (Figures 3B; $p = 0.862$, $t = -0.17$, $df = 45$; Table S1), although a strong tendency to track the object's location was still observed ($r = 0.80$, Figure 3A, bottom columns 1 and 2; also refer to Figure S3).

In contrast, males showed no steering response to the smaller 15° object ($p = 0.068$, $t = 1.87$, $df = 45$), even when it was coupled with acoustic cues (Figure 3A, column 3; female tone: $p = 0.462$, $t = -0.74$, $df = 46$; male tone: $p = 0.651$, $t = 0.45$, $df = 47$). These responses were indistinguishable from the control conditions where a static starfield, without any moving object, was presented with and without acoustic cues (Figures 3A, column 4, and 3B; no sound: $p = 0.121$, $t = 1.57$, $df = 96$; female tone: $p = 0.85$, $t = -0.18$, $df = 122$; male tone: $p = 0.90$, $t = -0.13$, $df = 118$; Table S2). Together, these results reveal a size-dependent threshold in mosquito visual-acoustic integration, suggesting that acoustic stimuli gate male responses to visual objects, such as other mosquitoes, only when they are in very close proximity.

Mosquitoes adjust their wing kinematics in response to visual cues

Contrary to our initial expectation that mosquitoes would steer away from visual objects as a collision-avoidance response, our observations did not support this behavior. This led us to further examine the effect of visual cues on mosquito responses beyond steering. We expanded our analysis to encompass changes in wing kinematics, specifically total wingbeat amplitude (L + R WBA) and wingbeat frequency (WBF), as males were presented with visual objects of varying sizes in the presence and absence of acoustic cues. WBA and WBF modulations allow flying insects to adjust the aerodynamic thrust forces required for performing flight maneuvers,[41–43] and thus this investigation aimed to determine whether visual information could influence other flight behaviors that can potentially contribute to collision-avoidance strategies.

Our analysis revealed a distinct pattern of modulation in wing kinematics. Males exhibited a decrease in both WBA and WBF as the visual object approached their frontal field of view, indicated by a negative correlation between the object's location and aerodynamic thrust production (Figure 4A, columns 1–3). Conversely, a monotonic increase in WBA and WBF was observed as the object moved away, indicated by a strong positive correlation in the subsequent temporal window (Figure 4A, columns 1–3). This response pattern was observed regardless of whether the visual objects were presented with or without acoustic cues (cf. Figure 4A, top, middle, and bottom rows) and was quite distinct from the control condition (static starfield without any object), where the responses remained unchanged or decreased monotonically (Figure 4A, column 4).

The observed modulation in WBAs in relation to the object's position was statistically significant across all acoustic treatments (no sound, female tone, male tone) and object sizes (37.5°, 22.5°, and 15°), confirming that this was a visually driven behavior (Figures 4B and S4; Tables S3 and S4). The modulation in WBF was also similar to WBA modulations (Figures 4C and S5; Table S5). While the changes in WBF for the 15° object were not statistically significant overall, the modulation pattern was still significantly different from the no-object control condition (Table S6). Interestingly, the extent of modulation in thrust production, resulting from the combined WBA and WBF adjustments, varied with object size, with the most drastic changes occurring in response to the largest (37.5°) visual stimulus (Figures 4B and 4C; Tables S4 and S6).

Subsequent experiments on female *An. coluzzii*, involving only visual stimuli without acoustic cues, revealed a similar modulation pattern across all three object sizes (Figure S6). Together, these results suggest that mosquitoes are capable of maneuvering in response to visual objects by adjusting their wingbeat kinematics, potentially utilizing this sensorimotor mechanism as a means to avoid collisions.

Collision-avoidance behavior of male mosquitoes flying freely in swarms

Our controlled virtual arena experiments suggest that tethered mosquitoes modify their flight patterns in response to visual objects simulating other mosquitoes at close range. To understand if these behavioral patterns found in tethered experiments also reflect free-flight patterns in natural swarming scenarios, we analyzed free-flight dynamics within *An. coluzzii* swarms (Figure 5A).[44] Given that the swarms of this species are predominantly male and it is challenging to identify the sex of individual mosquitoes in a swarm using current videography methods, our laboratory swarms were composed entirely of males. Across the six recorded swarming events,[44] the mosquito densities were low, with only 13 to 27 males swarming over a 40 × 40 cm ground marker. The average distance to the nearest neighbor in this dataset was 12.23 cm, with instances of close encounters within 2 cm constituting less than 1% of all nearest-neighbor distances within the swarm (Figure 5B). Considering that the wingspan of *Anopheles* mosquitoes is roughly 0.6 cm,[45] another mosquito within 2 cm would subtend a visual angle greater than 16.7°. This particular measure of proximity is especially relevant as it provides a benchmark to correlate the flight patterns observed in the controlled tethered setting with behaviors manifested during free flight.

First, we looked for evidence of collision avoidance in our dataset. Based on our tethered experiments, we expect mosquitoes may prevent collisions with visual objects by modulating their aerodynamic thrust-based forces. We therefore sought evidence for change in such forces when freely swarming mosquitoes flew in close proximity to each other. Inspired by research on other swarming species like midges and schooling fish in which interactions between individuals in a social group were modeled as effective forces,[46,47] we looked at whether mosquitoes tend to attract or repel each other by measuring the instantaneous acceleration of each mosquito toward its nearest neighbor. Here, positive and negative acceleration would signify attraction toward and repulsion from the nearest neighbor, respectively.

Our analysis indicated a clear "repulsion zone": on average, when mosquitoes were within 1.55 cm of each other (~2.5 body lengths), they accelerated away from their neighbor (negative accelerations), suggesting an intrinsic mechanism to prevent collisions (Figure 5C). Conversely, at larger distances, we noted

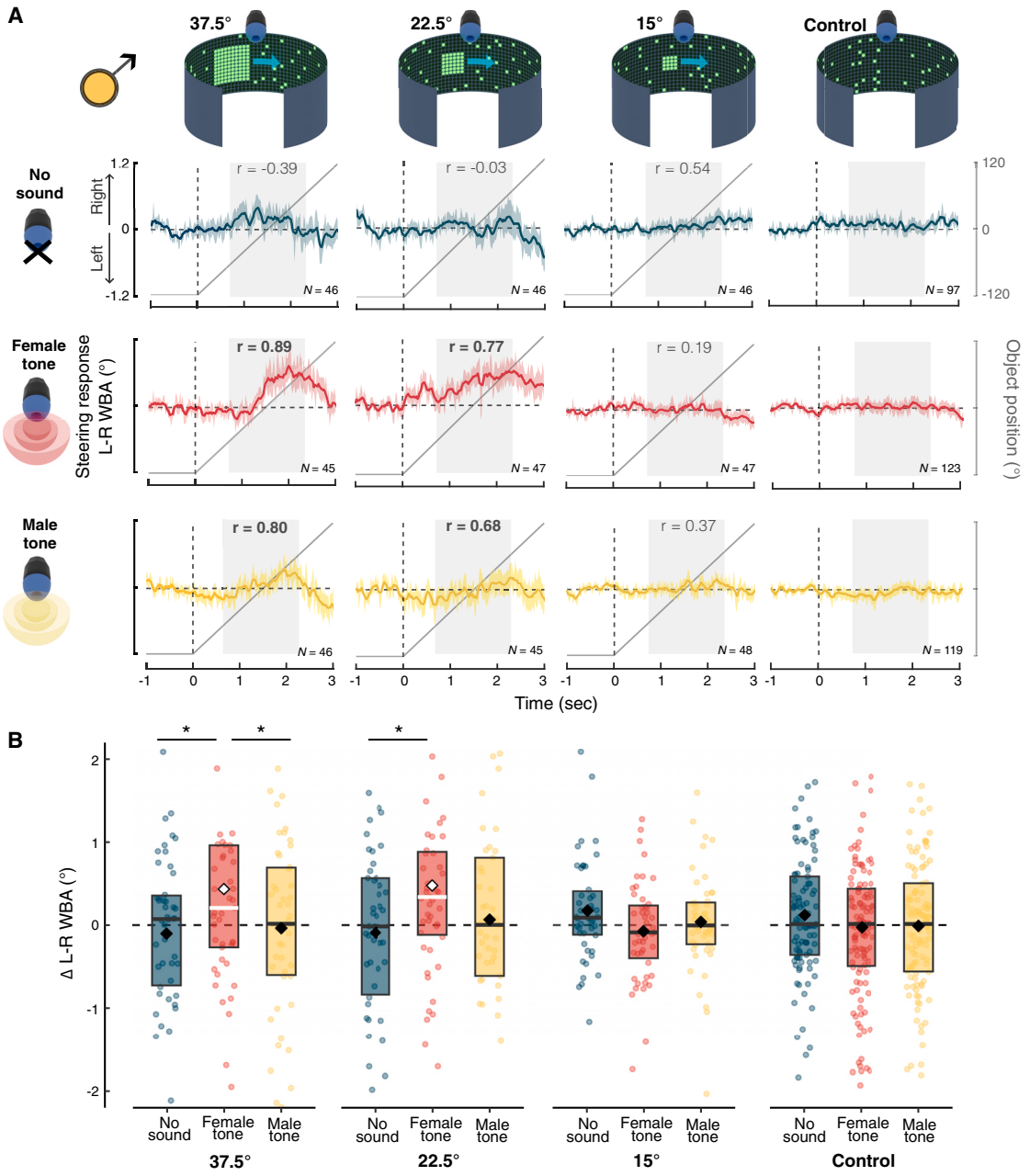

Figure 3. Size-dependent acoustic modulation of visual tracking in males

(A) Mean normalized steering responses of males to horizontally moving objects of three different sizes (37.5°, 22.5° referenced from Figure 2 for comparison, and 15°). For each object size, responses are measured under three conditions: without acoustic cue (row 1), in the presence of a female tone (row 2), and in the presence of a male tone (row 3). The solid gray line indicates the position of object, with 0° representing it directly in front of the mosquito. r value on each plot indicates Spearman's correlation between average steering response and the object position during the time segment highlighted by light gray shaded region. Values highlighted in bold signify moderate to strong correlation ($r > 0.6$). A control condition (column 4) with only the starfield pattern (no moving object) with and without acoustic cues was also tested. The full dynamics of steering responses before, during, and after stimulus presentation for each stimulus treatment can be seen in Figure S3.

(B) Statistical analysis of responses, shown via boxplots, quantifies the change in steering response from a pre-stimulus baseline to stimulus presentation. Boxplot elements include the interquartile range (box boundaries), mean (diamond), and median (horizontal line), with individual data points that fall within at least 95% quantile range. Mean and median symbols are color coded with white symbols and lines denoting statistical significance. Asterisks (*) denote significant differences between treatments obtained using a linear mixed-effect model (refer to Tables S1 and S2).

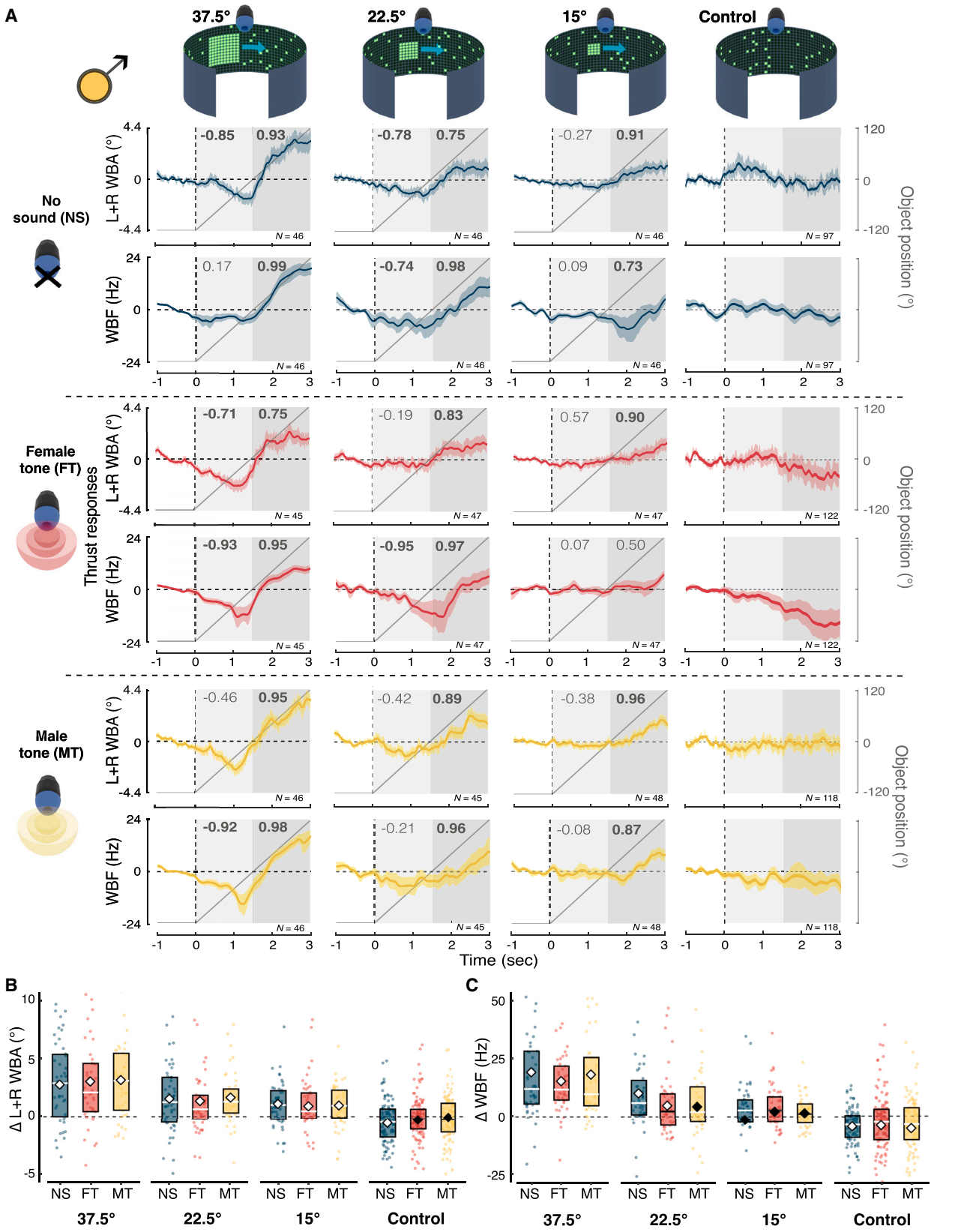

(legend on next page)

a pattern of increasing acceleration toward the nearest neighbor, which is a characteristic pattern that emerges when swarming individuals remain in the swarm.[47] To validate that the observed flight dynamics were influenced by the presence of a neighboring mosquito and were not simply a result of inherent flight patterns during swarming, we performed a hypothetical experiment using the same swarming dataset, but whereby we projected each focal mosquito 1 s into the future (Figure 5C). This allowed us to create a control dataset consisting of the flight dynamics of a virtual mosquito in relation to its apparent nearest neighbors. Analysis of this control dataset revealed a positive average acceleration of virtual mosquitoes toward their apparent neighbors at all distances, and thus on average no repulsion was observed from the control (Figure 5C). At neighbor distances smaller than 4 cm, the mosquitoes in the real data showed significantly lower accelerations toward their neighbors than the control (0–2 cm: $p = 0.008$, $\beta = -0.001$, SE = 0.0004; 2–4 cm: $p = 0.039$, $\beta = -0.0003$, SE = 0.0001, $df = 616{,}271$, linear mixed-effect model with log-transformed dependent variable). In contrast, at distances larger than 4 cm, accelerations were not significantly different between the real and control mosquitoes (4–6 cm: $p = 0.296$, $\beta = -0.00002$, SE = 0.0001, $df = 616{,}271$). Together, this analysis shows that male mosquitoes actively avoid collisions during close encounters.

Further analysis indicated that male mosquitoes modulated their thrust responses during close encounters by increasing their absolute acceleration (Figure 5D, left column). Statistical comparison with the control scenario validated that the observed increase in |acceleration| directly resulted from interaction with neighbors in close proximity (refer to Table S7). Interesting, while flight speed remained consistent across nearest-neighbor distances, both in real and control scenarios, mosquitoes in real swarms exhibited an increase in angular velocity (Figure 5D; Table S7), suggesting that males adjust their flight path or position rather than speed to evade each other.

Mosquitoes and fruit flies have been shown to evade large, looming objects using sharp directional evasive maneuvers.[48–50] However, our results suggest that sharp directional changes away from the neighbor may not be the strategy males use to avoid collisions in swarms. Mosquitoes did not significantly alter their flight direction relative to the position of their nearest neighbor compared with virtual mosquitoes (Figure 5D, right column; Table S7). This finding aligns with our observations from tethered-flight experiments, which demonstrated that males do not actively steer away from objects representing other males.

DISCUSSION

For swarming mosquitoes, acoustic sensing has long been the focal point of our understanding of inter-individual interactions, possibly overshadowing the importance of other sensory cues. This study broadens the current perspective by exploring the potential role of vision in shaping conspecific interactions within mating swarms. We discovered that *An. coluzzii* mosquitoes can detect and respond to visual objects representative of other mosquitoes, but their visual response is modulated by the sex-specific flight tones. Particularly, males exhibited a strong directional response to visual objects associated with female tones, indicating the integration of visual and acoustic signals to intercept females. Additionally, we found that visual cues alone were sufficient to trigger changes in wingbeat kinematics, potentially aiding in collision avoidance through subtle flight modifications. Many of the behavioral patterns we found in tethered experiments were supported by free-flight dynamics of swarming mosquitoes, providing compelling evidence in support of our hypothesis that *Anopheles* mosquitoes utilize visual cues of flying individuals in conjunction with acoustic information to approach potential mates and avoid collisions with conspecifics.

A growing body of research has documented the importance of visual cues for mosquitoes in various contexts, including host localization,[23,25,26] swarm formation,[51,52] and threat avoidance.[49,53] However, no published study has investigated the potential contribution of visual cues in mating behaviors and interactions with other conspecifics occurring within swarms. Our work has filled this gap by demonstrating that swarm-forming mosquitoes can not only respond to visual cues of conspecifics within mating swarms but also integrate these cues with acoustic signals to facilitate mating interactions.

We interpret our findings on visuo-acoustic integration to suggest that mosquitoes use visual cues of other flying mosquitoes as a supplementary aid alongside acoustic cues for interacting with nearby individuals, especially potential mates. Specifically, we propose that male mosquitoes, after identifying a potential mate through her flight tones, intercept her by using a phase-advanced steering response and following her flight trajectory. This sensory strategy is particularly relevant when males rapidly modulate their WBF while chasing females[18,54]—a behavior that can reduce the detectability of female flight tones due to changes in distortion product generation.[21] Distortion products, arising due to the nonlinear mixing of male and female flight tones within the mosquito's auditory system, are known to

Figure 4. Modulation of male wingbeat kinematics in response to object motion

(A) Normalized mean thrust responses of male mosquitoes, as indicated by total wingbeat amplitude (L + R WBA) and wingbeat frequency (WBF) in response to visual objects of three different sizes (37.5°, 22.5°, and 15°). For each object size, responses are measured under three conditions: without acoustic cue, in the presence of a female tone, and in the presence of a male tone. The solid gray line indicates the position of object, with 0° representing it directly in front of the mosquito. Numbers at the top of the gray colored segments indicates Spearman's correlation between average wing kinematics and the object position during the time segments highlighted by gray shaded regions. Values highlighted in bold signify moderate to strong correlation ($r > 0.6$). A control condition (column 4) with only the starfield pattern (no moving object) with and without acoustic cues was also tested. The full dynamics of wing kinematics for males and females before, during, and after stimulus presentation for each object size across the acoustic treatments can be seen in Figures S4–S6.

(B and C) (B) Statistical analysis of wingbeat amplitude responses and (C) wingbeat frequency responses, shown via boxplots, quantifies the difference in response across acoustic treatments as the object moves to the front (0–1.5 s) and as it moves away from the front (1.5–3 s). Boxplot elements include the interquartile range (box boundaries), mean (diamond), and median (horizontal line), with individual data points that fall within at least 95% quantile range. Mean and median symbols and lines are color coded with white denoting statistical significance obtained using t tests (refer to Tables S3 and S5). Statistical differences in thrust responses among objects of different sizes obtained using a linear mixed-effect model, are detailed in Tables S4 and S6.

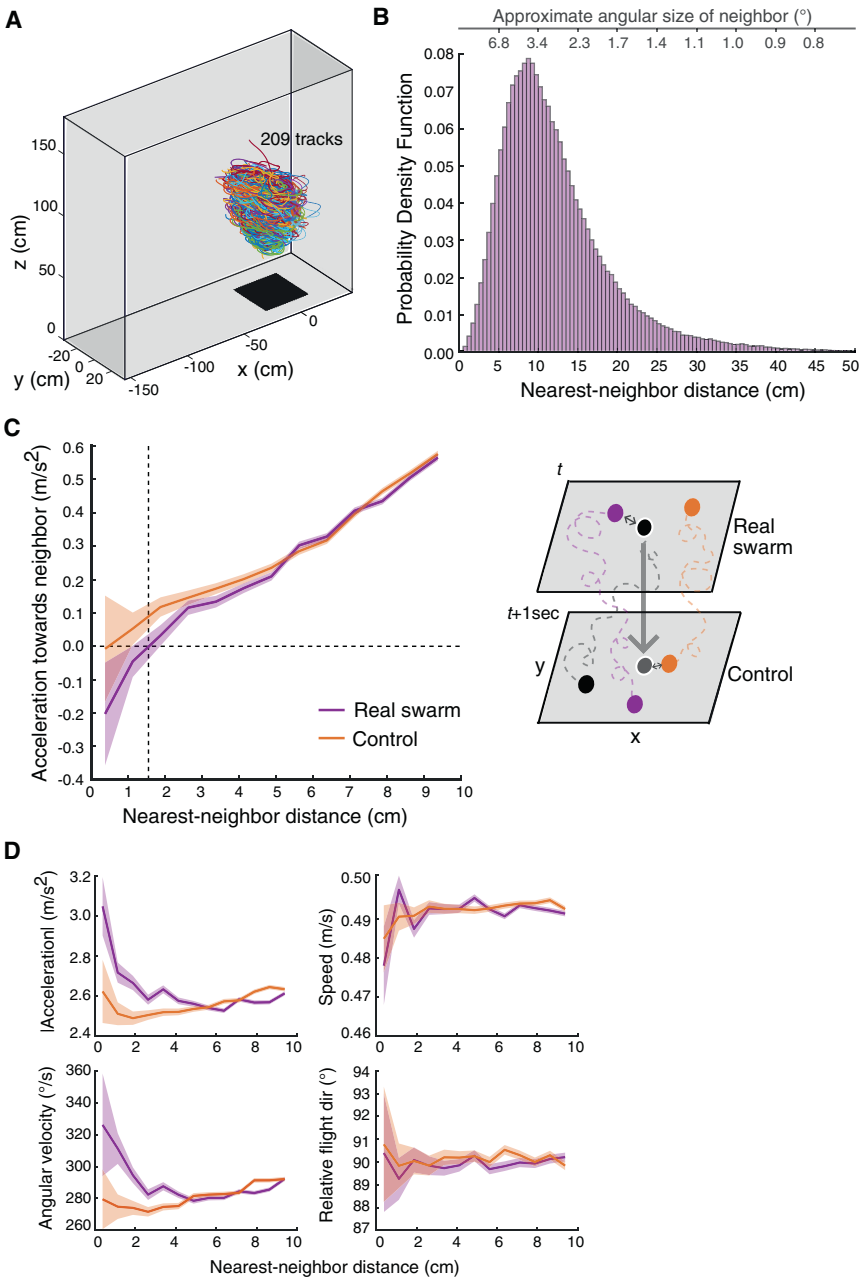

Figure 5. Analysis of flight dynamics as a function of nearest-neighbor distances in male swarms

(A) Flight trajectories of male *An. coluzzii* within a laboratory-generated swarm. The illustrated swarming event includes 25 mosquitoes, recorded for 150 s and resulting in 209 recorded tracks.

(B) Probability density function of nearest-neighbor distances across the six swarms (938 total trajectories). The gray scale at the top represents the approximate angular size of a neighboring mosquito at the corresponding distances (bottom x axis).

(C) (Left) Plot of acceleration of mosquitoes toward their nearest neighbor as a function of distance. Acceleration here is calculated by projecting the focal mosquito's acceleration onto the direction of its nearest neighbor, measuring the extent of repulsive and attractive forces between mosquitoes. Real swarm data (with n = 311,631 frames in which nearest-neighbor pairs were calculated) are represented in purple, while control data (with n = 304,657 frames) are in orange. (Right) Schematic representation of real swarm interactions (focal mosquito in black at time t with its nearest neighbor in purple) and hypothetical interactions in control data (focal mosquito projected to time t + 1 s in gray with its new nearest neighbor in orange at t + 1 s).

(D) Relationship between various flight parameters of mosquitoes (absolute acceleration, angular velocity, flight speed, and flight direction relative to their nearest neighbor) as a function of nearest-neighbor distances. Statistical differences between flight parameters at different nearest-neighbor distances in real swarm versus control data are noted in Table S7.

mediate acoustic detection of females.[19,55,56] Thus, as a male mosquito changes its WBF, its ability to detect these distortion products, and thereby the female, also changes, potentially making visual cues crucial for accurately intercepting the female during flight. Additionally, our results suggest that females likely utilize visual and acoustic cues not to actively follow but rather to orient themselves toward a nearby male. This observation aligns with the established mating dynamic in mosquitoes, where males are the primary pursuers of potential mates.[57,58] Lastly, our results show some correspondence between males' steering responses and the visual representation of a nearby male, supporting the notion of male-male interactions beyond simple avoidance, as previously suggested.[59–61]

The integration of visual and acoustic stimuli in *An. coluzzii* not only highlights a unique behavioral adaptation but also raises intriguing questions about the underlying neural mechanisms. Given the greater sensitivity of male mosquitoes to potential mates' flight tones,[13,19,62] and the alignment of steering magnitudes with known acoustic sensitivities of both sexes, it is reasonable to assume that information processing by the auditory system significantly influences mosquitoes' visual responses. The manner in which acoustic inputs modulate visual processing pathways presents an intriguing subject for future research. Existing literature suggests that neuromodulators are critical to shaping the output of insect neural circuits and altering their behavioral states.[63–65] In mosquitoes, the neuromodulator octopamine has been shown to play an integral role in auditory function[66] providing efferent feedback to the Johnston's organ via octopaminergic neurons.[67] Interestingly, these neurons also project to the lobula region of the optic lobe, where "object selective" neurons known to process small-field visual information are typically present in insects.[30,68] This convergence of auditory and visual neural

pathways, and innervation by neuromodulator-expressing cells, suggests a potential neural basis for visual-auditory integration.[27] Investigating the neural pathways and the role of neuromodulators across sensory systems could provide insights into the mechanism of sensory integration, potentially offering novel avenues for vector control strategies.

Beyond the integration of visual and acoustic cues, our study also sheds light on the independent influence of small visual objects on mosquito behavior. Distinct from responses in other Diptera—such as rigidly tethered *Drosophila melanogaster*, which steers away from objects smaller than 30°,[69,70] and *Aedes aegypti*, which steer toward these objects[30]—*An. coluzzii* demonstrates a unique response. Instead of differentially modulating their left and right WBA in response to moving visual objects to steer in yaw direction, *Anopheles* mosquitoes modulated other wingbeat kinematics, specifically total WBA and WBF. This modulation was not dependent on acoustic stimuli and varied with the size of the visual object, suggesting that this is a purely visual-driven mechanism that mosquitoes might be using to avoid collisions with nearby mosquitoes in a swarm. Our free-flight data support these results, showing that mosquitoes manage close encounters not by making strong directional changes away from neighbors but by adjusting their angular velocity and acceleration, which might appear in a swarm as quick, scall-scale adjustments in position through a descent or ascent, or subtle shifts in direction. However, to fully decode the kinematics of mosquito collision avoidance with conspecifics, future research should employ high-speed videography to capture responses to small, looming targets.

In conclusion, this study broadens our understanding of mosquito sensory ecology by highlighting the significance of visual cues and the integration of visual and acoustic cues in shaping interactions among conspecifics. Our findings offer compelling evidence that mosquitoes actively process and integrate visual and acoustic information, a discovery that has implications for both ecological research and public health initiatives, particularly in the context of vector control. Notably, understanding these sensory interactions might inform the design of more effective interventions. For example, augmenting acoustic lures, which have shown variable effectiveness under natural conditions[71–73], with long-range visual cues such as high-contrast patterns could potentially improve their attractiveness. Employing such multisensory lure and trap methods could lead to more efficient methods for capturing and monitoring swarming mosquitoes, potentially reducing the labor-intensive swarm trapping methods.

STAR★METHODS

Detailed methods are provided in the online version of this paper and include the following:

SUPPLEMENTAL INFORMATION

Supplemental information can be found online at https://doi.org/10.1016/j.cub.2024.07.043.

ACKNOWLEDGMENTS

We thank Simon Sawadogo for sharing pictures of natural swarms; Ruth Müller, Simon Sawadogo, Sofia Vielma, and members of the Riffell lab for feedback on this work; Binh Nguyen and Nicolas Avendano for helping with mosquito care; and Mridul Yadav for making the illustrations. This work was supported by grants from the Human Frontiers Science Program (HFSP -RGP0044/2021), the National Institutes of Health (R01AI148300 and R01AI175152), the Air Force Office of Scientific Research (FA9550-21-1-0101 and AWD-004055-G4), and the French National Research Agency (ANR-15-CE35-0001-01).

AUTHOR CONTRIBUTIONS

Conceptualization, S.G. and J.A.R.; methodology, S.G. and J.A.R.; investigation, S.G. and S.B.P.; analysis, S.G. and A.C.; writing – original draft, S.G.; writing – review and editing, S.G., J.A.R., F.T.M., S.B.P., A.C., and O.R.; funding acquisition, J.A.R., F.T.M., and O.R.

DECLARATION OF INTERESTS

The authors declare no competing interests.

Received: April 30, 2024
Revised: July 1, 2024
Accepted: July 11, 2024
Published: August 30, 2024

REFERENCES

1. Kirkpatrick, M., and Ryan, M.J. (1991). The evolution of mating preferences and the paradox of the lek. Nature *350*, 33–38. https://doi.org/10.1038/350033a0.
2. Rathore, A., Isvaran, K., and Guttal, V. (2023). Lekking as collective behaviour. Philos. Trans. R. Soc. Lond. B Biol. Sci. *378*, 20220066. https://doi.org/10.1098/rstb.2022.0066.
3. Shelly, T.E., and Whittier, T.S. (1997). Lek behavior of insects. In The Evolution of Mating Systems in Insects and Arachnids, B.J. Crespi, and J.C. Choe, eds. (Cambridge University Press), pp. 273–293. https://doi.org/10.1017/CBO9780511721946.017.
4. Allan, J.D., and Flecker, A.S. (1989). The mating biology of a mass-swarming mayfly. Anim. Behav. *37*, 361–371. https://doi.org/10.1016/0003-3472(89)90084-5.
5. Newkirk, M.R. (1970). Biology of the Longtailed Dance Fly, *Rhamphomyia longicauda* (Diptera: Enipididae); a New Look at Swarming1. Ann. Entomol. Soc. Am. *63*, 1407–1412. https://doi.org/10.1093/aesa/63.5.1407.
6. Downes, J.A. (1969). The Swarming and Mating Flight of Diptera. Annu. Rev. Entomol. *14*, 271–298. https://doi.org/10.1146/annurev.en.14.010169.001415.

7. Charlwood, J.D. (2023). Swarming and mate selection in *Anopheles gambiae* mosquitoes (Diptera: Culicidae). J. Med. Entomol. *60*, 857–864. https://doi.org/10.1093/jme/tjad064.

8. Sawadogo, S.P., Niang, A., Bilgo, E., Millogo, A., Maïga, H., Dabire, R.K., Tripet, F., and Diabaté, A. (2017). Targeting male mosquito swarms to control malaria vector density. PLOS ONE *12*, e0173273. https://doi.org/10.1371/journal.pone.0173273.

9. Dahalan, F.A., Churcher, T.S., Windbichler, N., and Lawniczak, M.K.N. (2019). The male mosquito contribution towards malaria transmission: Mating influences the *Anopheles* female midgut transcriptome and increases female susceptibility to human malaria parasites. PLOS Pathog. *15*, e1008063. https://doi.org/10.1371/journal.ppat.1008063.

10. Charlwood, J.D., and Jones, M.D.R. (1980). Mating in the mosquito, *Anopheles gambiae* s.l. Physiol. Entomol. *5*, 315–320. https://doi.org/10.1111/j.1365-3032.1980.tb00241.x.

11. Sawadogo, P.S., Namountougou, M., Toé, K.H., Rouamba, J., Maïga, H., Ouédraogo, K.R., Baldet, T., Gouagna, L.C., Kengne, P., Simard, F., et al. (2014). Swarming behaviour in natural populations of *Anopheles gambiae* and *An. coluzzii*: Review of 4 years survey in rural areas of sympatry, Burkina Faso (West Africa). Acta Trop. *132*, S42–S52. https://doi.org/10.1016/j.actatropica.2013.12.011.

12. Baeshen, R. (2022). Swarming Behavior in *Anopheles gambiae* (sensu lato): Current Knowledge and Future Outlook. J. Med. Entomol. *59*, 56–66. https://doi.org/10.1093/jme/tjab157.

13. Göpfert, M.C., and Robert, D. (2000). Nanometre–range acoustic sensitivity in male and female mosquitoes. Proc. Biol. Sci. *267*, 453–457. https://doi.org/10.1098/rspb.2000.1021.

14. Su, M.P., Andrés, M., Boyd-Gibbins, N., Somers, J., and Albert, J.T. (2018). Sex and species specific hearing mechanisms in mosquito flagellar ears. Nat. Commun. *9*, 3911. https://doi.org/10.1038/s41467-018-06388-7.

15. Belton, P. (1994). Attraction of male mosquitoes to sound. J. Am. Mosq. Control Assoc. *10*, 297–301.

16. Andrés, M., Su, M.P., Albert, J., and Cator, L.J. (2020). Buzzkill: targeting the mosquito auditory system. Curr. Opin. Insect Sci. *40*, 11–17. https://doi.org/10.1016/j.cois.2020.04.003.

17. Göpfert, M.C., Briegel, H., and Robert, D. (1999). Mosquito hearing: sound-induced antennal vibrations in male and female *Aedes aegypti*. J. Exp. Biol. *202*, 2727–2738. https://doi.org/10.1242/jeb.202.20.2727.

18. Simões, P.M.V., Ingham, R.A., Gibson, G., and Russell, I.J. (2016). A role for acoustic distortion in novel rapid frequency modulation behaviour in free-flying male mosquitoes. J. Exp. Biol. *219*, 2039–2047. https://doi.org/10.1242/jeb.135293.

19. Simões, P.M.V., Ingham, R., Gibson, G., and Russell, I.J. (2018). Masking of an auditory behaviour reveals how male mosquitoes use distortion to detect females. Proc. Biol. Sci. *285*, 20171862. https://doi.org/10.1098/rspb.2017.1862.

20. Lapshin, D.N., and Vorontsov, D.D. (2021). Frequency tuning of swarming male mosquitoes (*Aedes communis*, Culicidae) and its neural mechanisms. J. Insect Physiol. *132*, 104233. https://doi.org/10.1016/j.jinsphys.2021.104233.

21. Somers, J., Georgiades, M., Su, M.P., Bagi, J., Andrés, M., Alampounti, A., Mills, G., Ntabaliba, W., Moore, S.J., Spaccapelo, R., and Albert, J.T. (2022). Hitting the right note at the right time: Circadian control of audibility in *Anopheles* mosquito mating swarms is mediated by flight tones. Sci. Adv. *8*, eabl4844. https://doi.org/10.1126/sciadv.abl4844.

22. McMeniman, C.J., Corfas, R.A., Matthews, B.J., Ritchie, S.A., and Vosshall, L.B. (2014). Multimodal Integration of Carbon Dioxide and Other Sensory Cues Drives Mosquito Attraction to Humans. Cell *156*, 1060–1071. https://doi.org/10.1016/j.cell.2013.12.044.

23. van Breugel, F., Riffell, J., Fairhall, A., and Dickinson, M.H. (2015). Mosquitoes Use Vision to Associate Odor Plumes with Thermal Targets. Curr. Biol. *25*, 2123–2129. https://doi.org/10.1016/j.cub.2015.06.046.

24. Carnaghi, M., Belmain, S.R., Hopkins, R.J., and Hawkes, F.M. (2021). Multimodal synergisms in host stimuli drive landing response in malaria mosquitoes. Sci. Rep. *11*, 7379. https://doi.org/10.1038/s41598-021-86772-4.

25. Alonso San Alberto, D., Rusch, C., Zhan, Y., Straw, A.D., Montell, C., and Riffell, J.A. (2022). The olfactory gating of visual preferences to human skin and visible spectra in mosquitoes. Nat. Commun. *13*, 555. https://doi.org/10.1038/s41467-022-28195-x.

26. Hawkes, F., and Gibson, G. (2016). Seeing is believing: the nocturnal malarial mosquito *Anopheles coluzzii* responds to visual host-cues when odour indicates a host is nearby. Parasit. Vectors *9*, 320. https://doi.org/10.1186/s13071-016-1609-z.

27. Gupta, S., and Riffell, J.A. (2022). Sensory neurophysiology and integration in mosquitoes. Chapter 30. In Sensory Ecology of Disease Vectors, R. Ignell, C.R. Lazzari, M.G. Lorenzo, and S.R. Hill, eds. (Wageningen Academic Publishers), pp. 773–799. https://doi.org/10.3920/978-90-8686-932-9_30.

28. Land, M.F., Gibson, G., and Horwood, J. (1997). Mosquito Eye Design: Conical Rhabdoms are Matched to Wide Aperture Lenses. Proc. R. Soc. Lond. B *264*, 1183–1187. https://doi.org/10.1098/rspb.1997.0163.

29. Gonzalez-Bellido, P.T., Fabian, S.T., and Nordström, K. (2016). Target detection in insects: optical, neural and behavioral optimizations. Curr. Opin. Neurobiol. *41*, 122–128. https://doi.org/10.1016/j.conb.2016.09.001.

30. Vinauger, C., Van Breugel, F., Locke, L.T., Tobin, K.K.S., Dickinson, M.H., Fairhall, A.L., Akbari, O.S., and Riffell, J.A. (2019). Visual-Olfactory Integration in the Human Disease Vector Mosquito *Aedes aegypti*. Curr. Biol. *29*, 2509–2516.e5. https://doi.org/10.1016/j.cub.2019.06.043.

31. Bartussek, J., and Lehmann, F.-O. (2016). Proprioceptive feedback determines visuomotor gain in *Drosophila*. R. Soc. Open Sci. *3*, 150562. https://doi.org/10.1098/rsos.150562.

32. Duistermars, B.J., Reiser, M.B., Zhu, Y., and Frye, M.A. (2007). Dynamic properties of large-field and small-field optomotor flight responses in Drosophila. J. Comp. Physiol. A Neuroethol. Sens. Neural Behav. Physiol. *193*, 787–799. https://doi.org/10.1007/s00359-007-0233-y.

33. Ellington, C.P. (1984). The Aerodynamics of Hovering Insect Flight. IV. Aerodynamic Mechanisms. Philos. Trans. R. Soc. Lond. B *305*, 79–113.

34. Gibson, G., and Russell, I. (2006). Flying in Tune: Sexual Recognition in Mosquitoes. Curr. Biol. *16*, 1311–1316. https://doi.org/10.1016/j.cub.2006.05.053.

35. Pennetier, C., Warren, B., Dabiré, K.R., Russell, I.J., and Gibson, G. (2010). "Singing on the Wing" as a Mechanism for Species Recognition in the Malarial Mosquito *Anopheles gambiae*. Curr. Biol. *20*, 131–136. https://doi.org/10.1016/j.cub.2009.11.040.

36. Feugère, L., Gibson, G., Manoukis, N.C., and Roux, O. (2021). Mosquito sound communication: are male swarms loud enough to attract females? J. R. Soc. Interface *18*, 20210121. https://doi.org/10.1098/rsif.2021.0121.

37. Su, M.P., Georgiades, M., Bagi, J., Kyrou, K., Crisanti, A., and Albert, J.T. (2020). Assessing the acoustic behaviour of *Anopheles gambiae* (s.l.) dsxF mutants: implications for vector control. Parasit. Vectors *13*, 507. https://doi.org/10.1186/s13071-020-04382-x.

38. Rimniceanu, M., Currea, J.P., and Frye, M.A. (2023). Proprioception gates visual object fixation in flying flies. Curr. Biol. *33*, 1459–1471.e3. https://doi.org/10.1016/j.cub.2023.03.018.

39. Cellini, B., Ferrero, M., and Mongeau, J.-M. (2024). *Drosophila* flying in augmented reality reveals the vision-based control autonomy of the optomotor response. Curr. Biol. *34*, 68–78.e4. https://doi.org/10.1016/j.cub.2023.11.045.

40. Keleş, M.F., Mongeau, J.-M., and Frye, M.A. (2019). Object features and T4/T5 motion detectors modulate the dynamics of bar tracking by Drosophila. J. Exp. Biol. *222*, jeb190017. https://doi.org/10.1242/jeb.190017.

41. Olejnik, D.A., Muijres, F.T., Karásek, M., Honfi Camilo, L., De Wagter, C., and de Croon, G.C.H.E. (2022). Flying Into the Wind: Insects and

Bio-Inspired Micro-Air-Vehicles With a Wing-Stroke Dihedral Steer Passively Into Wind-Gusts. Front. Robot. AI *9*, 820363. https://doi.org/10.3389/frobt.2022.820363.

42. Lehmann, F.O., and m, M.H. (1998). The Control of Wing Kinematics And Flight Forces In Fruit Flies (*Drosophila* Spp.). J. Exp. Biol. *201*, 385–401. https://doi.org/10.1242/jeb.201.3.385.
43. Van Veen, W.G., Van Leeuwen, J.L., Van Oudheusden, B.W., and Muijres, F.T. (2022). The unsteady aerodynamics of insect wings with rotational stroke accelerations, a systematic numerical study. J. Fluid Mech. *936*, A3. https://doi.org/10.1017/jfm.2022.31.
44. Poda, B.S., Cribellier, A., Feugère, L., Fatou, M., Nignan, C., Hien, D.F.de S., Müller, P., Gnankiné, O., Dabiré, R.K., Diabaté, A., et al. (2024). Spatial and temporal characteristics of laboratory-induced *Anopheles coluzzii* swarms: shape, structure and flight kinematics. Preprint at bioRxiv. https://doi.org/10.1101/2024.03.25.586329.
45. Niang, A., Sawadogo, S.P., Dabiré, R.K., Tripet, F., and Diabaté, A. (2020). Assessment of the ecologically dependent post-zygotic isolation between *Anopheles coluzzii* and *Anopheles gambiae*. PLoS One *15*, e0240625. https://doi.org/10.1371/journal.pone.0240625.
46. Katz, Y., Tunstrøm, K., Ioannou, C.C., Huepe, C., and Couzin, I.D. (2011). Inferring the structure and dynamics of interactions in schooling fish. Proc. Natl. Acad. Sci. USA *108*, 18720–18725. https://doi.org/10.1073/pnas.1107583108.
47. Puckett, J.G., Kelley, D.H., and Ouellette, N.T. (2014). Searching for effective forces in laboratory insect swarms. Sci. Rep. *4*, 4766. https://doi.org/10.1038/srep04766.
48. Muijres, F.T., Elzinga, M.J., Melis, J.M., and Dickinson, M.H. (2014). Flies Evade Looming Targets by Executing Rapid Visually Directed Banked Turns. Science *344*, 172–177. https://doi.org/10.1126/science.1248955.
49. Cribellier, A., Straw, A.D., Spitzen, J., Pieters, R.P.M., van Leeuwen, J.L., and Muijres, F.T. (2022). Diurnal and nocturnal mosquitoes escape looming threats using distinct flight strategies. Curr. Biol. *32*, 1232–1246.e5. https://doi.org/10.1016/j.cub.2022.01.036.
50. Cribellier, A., Camilo, L.H., Goyal, P., and Muijres, F.T. (2024). Mosquitoes escape looming threats by actively flying with the bow wave induced by the attacker. Curr. Biol. *34*, 1194–1205.e7. https://doi.org/10.1016/j.cub.2024.01.066.
51. Poda, S.B., Nignan, C., Gnankiné, O., Dabiré, R.K., Diabaté, A., and Roux, O. (2019). Sex aggregation and species segregation cues in swarming mosquitoes: role of ground visual markers. Parasit. Vectors *12*, 589. https://doi.org/10.1186/s13071-019-3845-5.
52. Jain, P., Singh, O.P., and Butail, S. (2020). Dynamics of mosquito swarms over a moving marker. Preprint at arXiv. https://doi.org/10.48550/arXiv.2007.04254.
53. Wynne, N.E., Chandrasegaran, K., Fryzlewicz, L., and Vinauger, C. (2022). Visual threats reduce blood-feeding and trigger escape responses in *Aedes aegypti* mosquitoes. Sci. Rep. *12*, 21354. https://doi.org/10.1038/s41598-022-25461-2.
54. Simões, P.M.V., Gibson, G., and Russell, I.J. (2017). Pre-copula acoustic behaviour of males in the malarial mosquitoes *Anopheles coluzzii* and *Anopheles gambiae* s.s. does not contribute to reproductive isolation. J. Exp. Biol. *220*, 379–385. https://doi.org/10.1242/jeb.149757.
55. Warren, B., Gibson, G., and Russell, I.J. (2009). Sex Recognition through Midflight Mating Duets in *Culex* Mosquitoes Is Mediated by Acoustic Distortion. Curr. Biol. *19*, 485–491. https://doi.org/10.1016/j.cub.2009.01.059.
56. Arthur, B.J., Wyttenbach, R.A., Harrington, L.C., and Hoy, R.R. (2010). Neural responses to one- and two-tone stimuli in the hearing organ of the dengue vector mosquito. J. Exp. Biol. *213*, 1376–1385. https://doi.org/10.1242/jeb.033357.
57. Roth, L.M. (1948). A Study of Mosquito Behavior. An Experimental Laboratory Study of the Sexual Behavior of *Aedes aegypti* (Linnaeus). Am. Midl. Nat. *40*, 265–352. https://doi.org/10.2307/2421604.
58. Feugère, L., Simoes, P.M.V., Russell, I.J., and Gibson, G. (2022). The role of hearing in mosquito behaviour. Chapter 26. In Sensory Ecology of Disease Vectors, R. Ignell, C.R. Lazzari, M.G. Lorenzo, and S.R. Hill, eds. (Wageningen Academic Publishers), pp. 683–708. https://doi.org/10.3920/978-90-8686-932-9_26.
59. Shishika, D., Manoukis, N.C., Butail, S., and Paley, D.A. (2014). Male motion coordination in anopheline mating swarms. Sci. Rep. *4*, 6318. https://doi.org/10.1038/srep06318.
60. Pantoja-Sánchez, H., Gomez, S., Velez, V., Avila, F.W., and Alfonso-Parra, C. (2019). Precopulatory acoustic interactions of the New World malaria vector *Anopheles albimanus* (Diptera: Culicidae). Parasit. Vectors *12*, 386. https://doi.org/10.1186/s13071-019-3648-8.
61. Aldersley, A., Champneys, A., Homer, M., Bode, N.W.F., and Robert, D. (2017). Emergent acoustic order in arrays of mosquitoes. Curr. Biol. *27*, R1208–R1210. https://doi.org/10.1016/j.cub.2017.09.055.
62. Jackson, J.C., and Robert, D. (2006). Nonlinear auditory mechanism enhances female sounds for male mosquitoes. Proc. Natl. Acad. Sci. USA *103*, 16734–16739. https://doi.org/10.1073/pnas.0606319103.
63. Brezina, V. (2010). Beyond the wiring diagram: signalling through complex neuromodulator networks. Philos. Trans. R. Soc. Lond. B Biol. Sci. *365*, 2363–2374. https://doi.org/10.1098/rstb.2010.0105.
64. Su, C.-Y., and Wang, J.W. (2014). Modulation of neural circuits: how stimulus context shapes innate behavior in *Drosophila*. Curr. Opin. Neurobiol. *29*, 9–16. https://doi.org/10.1016/j.conb.2014.04.008.
65. Kamhi, J.F., Arganda, S., Moreau, C.S., and Traniello, J.F.A. (2017). Origins of Aminergic Regulation of Behavior in Complex Insect Social Systems. Front. Syst. Neurosci. *11*, 74. https://doi.org/10.3389/fnsys.2017.00074.
66. Georgiades, M., Alampounti, A., Somers, J., Su, M.P., Ellis, D.A., Bagi, J., Terrazas-Duque, D., Tytheridge, S., Ntabaliba, W., Moore, S., et al. (2023). Hearing of malaria mosquitoes is modulated by a beta-adrenergic-like octopamine receptor which serves as insecticide target. Nat. Commun. *14*, 4338. https://doi.org/10.1038/s41467-023-40029-y.
67. Andrés, M., Seifert, M., Spalthoff, C., Warren, B., Weiss, L., Giraldo, D., Winkler, M., Pauls, S., and Göpfert, M.C. (2016). Auditory Efferent System Modulates Mosquito Hearing. Current Biology *26*, 2028–2036. https://doi.org/10.1016/j.cub.2016.05.077.
68. Wasserman, S.M., Aptekar, J.W., Lu, P., Nguyen, J., Wang, A.L., Keles, M.F., Grygoruk, A., Krantz, D.E., Larsen, C., and Frye, M.A. (2015). Olfactory Neuromodulation of Motion Vision Circuitry in *Drosophila*. Curr. Biol. *25*, 467–472. https://doi.org/10.1016/j.cub.2014.12.012.
69. Maimon, G., Straw, A.D., and Dickinson, M.H. (2008). A Simple Vision-Based Algorithm for Decision Making in Flying Drosophila. Curr. Biol. *18*, 464–470. https://doi.org/10.1016/j.cub.2008.02.054.
70. Park, E.J., and Wasserman, S.M. (2018). Diversity of visuomotor reflexes in two Drosophila species. Curr. Biol. *28*, R865–R866. https://doi.org/10.1016/j.cub.2018.06.071.
71. Pantoja-Sánchez, H., Vargas, J.F., Ruiz-López, F., Rúa-Uribe, G., Vélez, V., Kline, D.L., and Bernal, X.E. (2019). A new approach to improve acoustic trapping effectiveness for *Aedes aegypti* (Diptera: Culicidae). J. Vector Ecol. *44*, 216–222. https://doi.org/10.1111/jvec.12352.
72. Johnson, B.J., Rohde, B.B., Zeak, N., Staunton, K.M., Prachar, T., and Ritchie, S.A. (2018). A low-cost, battery-powered acoustic trap for surveilling male *Aedes aegypti* during rear-and-release operations. PLoS One *13*, e0201709. https://doi.org/10.1371/journal.pone.0201709.
73. Staunton, K.M., Leiva, D., Cruz, A., Goi, J., Arisqueta, C., Liu, J., Desnoyer, M., Howell, P., Espinosa, F., Mendoza, A.C., et al. (2021). Outcomes from international field trials with Male *Aedes* Sound Traps: Frequency-dependent effectiveness in capturing target species in relation to bycatch abundance. PLOS Negl. Trop. Dis. *15*, e0009061. https://doi.org/10.1371/journal.pntd.0009061.
74. Reiser, M.B., and Dickinson, M.H. (2008). A modular display system for insect behavioral neuroscience. J. Neurosci. Methods *167*, 127–139. https://doi.org/10.1016/j.jneumeth.2007.07.019.

75. Cheng, K.Y., Colbath, R.A., and Frye, M.A. (2019). Olfactory and Neuromodulatory Signals Reverse Visual Object Avoidance to Approach in Drosophila. Curr. Biol. *29*, 2058–2065.e2. https://doi.org/10.1016/j.cub.2019.05.010.

76. Cellini, B., and Mongeau, J.-M. (2022). Nested mechanosensory feedback actively damps visually guided head movements in Drosophila. eLife *11*, e80880. https://doi.org/10.7554/eLife.80880.

77. Liu, M.Z., and Vosshall, L.B. (2019). General Visual and Contingent Thermal Cues Interact to Elicit Attraction in Female *Aedes aegypti* Mosquitoes. Curr. Biol. *29*, 2250–2257.e4. https://doi.org/10.1016/j.cub.2019.06.001.

78. Bomphrey, R.J., Nakata, T., Phillips, N., and Walker, S.M. (2017). Smart wing rotation and trailing-edge vortices enable high frequency mosquito flight. Nature *544*, 92–95. https://doi.org/10.1038/nature21727.

79. Suver, M.P., Huda, A., Iwasaki, N., Safarik, S., and Dickinson, M.H. (2016). An Array of Descending Visual Interneurons Encoding Self-Motion in *Drosophila*. J. Neurosci. *36*, 11768–11780. https://doi.org/10.1523/JNEUROSCI.2277-16.2016.

80. Nakata, T., Simões, P., Walker, S.M., Russell, I.J., and Bomphrey, R.J. (2022). Auditory sensory range of male mosquitoes for the detection of female flight sound. J. R. Soc. Interface *19*, 20220285. https://doi.org/10.1098/rsif.2022.0285.

81. Sawadogo, S.P., Costantini, C., Pennetier, C., Diabaté, A., Gibson, G., and Dabiré, R.K. (2013). Differences in timing of mating swarms in sympatric populations of *Anopheles coluzzii* and *Anopheles gambiae s.s.* (formerly *An. gambiae* M and S molecular forms) in Burkina Faso, West Africa. Parasit. Vectors *6*, 275. https://doi.org/10.1186/1756-3305-6-275.

82. Niang, A., Sawadogo, S.P., Millogo, A.A., Akpodiete, N.O., Dabiré, R.K., Tripet, F., and Diabaté, A. (2021). Entomological baseline data collection and power analyses in preparation of a mosquito swarm-killing intervention in south-western Burkina Faso. Malar. J. *20*, 346. https://doi.org/10.1186/s12936-021-03877-x.

83. Hawkes, F.M., Zeil, J., and Gibson, G. (2022). Vision in mosquitoes. Chapter 19. In Sensory Ecology of Disease Vectors, R. Ignell, C.R. Lazzari, M.G. Lorenzo, and S.R. Hill, eds. (Wageningen Academic), pp. 511–533. https://doi.org/10.3920/978-90-8686-932-9_19.

84. Feugère, L., Roux, O., and Gibson, G. (2022). Behavioural analysis of swarming mosquitoes reveals high hearing sensitivity in *Anopheles coluzzii*. J. Exp. Biol. *225*, jeb243535. https://doi.org/10.1242/jeb.243535.

85. Kwak, S.G., and Kim, J.H. (2017). Central limit theorem: the cornerstone of modern statistics. Korean J. Anesthesiol. *70*, 144–156. https://doi.org/10.4097/kjae.2017.70.2.144.

86. Schielzeth, H., Dingemanse, N.J., Nakagawa, S., Westneat, D.F., Allegue, H., Teplitsky, C., Réale, D., Dochtermann, N.A., Garamszegi, L.Z., and Araya-Ajoy, Y.G. (2020). Robustness of linear mixed-effects models to violations of distributional assumptions. Methods Ecol. Evol. *11*, 1141–1152. https://doi.org/10.1111/2041-210X.13434.

STAR★METHODS

KEY RESOURCES TABLE

REAGENT or RESOURCE	SOURCE	IDENTIFIER
Deposited data		
Dataset and code	This paper	http://www.doi.org/10.17632/tn4cpwbxpm.1
Experimental models: Organisms/strains		
Anopheles coluzzii Ngousso strain	BEI Resources	MRA-1279
Software and algorithms		
Kinefly	Custom	https://github.com/ssafarik/Kinefly
MATLAB R2023a	MathWorks	https://www.mathworks.com/products/matlab.html
R v4.3.1	R Development Core Team	https://www.r-project.org/
Other		
LED panel visual display system	Custom	Reiser and Dickinson[74]
Wingbeat Analyzer	JFI Electronics	N/A
Firefly USB camera	Point Grey Research	FMVU-03MTM-CS
Infrared bandpass filter	Midwest Optical Systems	BP800-25.4

RESOURCE AVAILABILITY

Lead contact

Further information and requests for resources should be directed to and will be fulfilled by the lead contact, Jeff Riffell (jriffell@uw.edu).

Materials availability

This study did not generate new unique reagents.

Data and code availability

The datasets and code supporting the analyses presented in this paper are publicly available at Mendeley Data: http://www.doi.org/10.17632/tn4cpwbxpm.1

EXPERIMENTAL MODEL AND SUBJECT DETAILS

We used 4- to 6-day-old unmated, wild-type *Anopheles coluzzii* (Ngousso strain, MRA-1279) as test subjects for the experiments with tethered mosquitoes. The colonies were reared in environment control chambers (Intellus, Pervical Scientific Inc., Perry, IA, USA), maintained at a temperature of 26±1°C and 60±10% relative humidity under a 12- hour light/12-hour dark cycle. To ensure that subjects remain unmated, we isolated individual pupae in 50-mL Falcon tubes each day. Upon emergence, adults were provided with cotton saturated with a 10% sucrose solution. Given that this species typically initiates swarming around dusk, all experiments were conducted during the first hour of the dark cycle to align with their natural swarming patterns. Furthermore, our controlled sensory experiments specifically included mosquitoes that displayed consistent flying while being tethered, ensuring their physiological state closely resembled that during swarming.

METHOD DETAILS

Tethering procedure

Subjects were anesthetized by brief exposure to cold for no more than 3 minutes before being placed on a Peltier cooling stage, maintained at approximately 4°C, to ensure they remained immobilized during tethering. Each individual was subsequently fixed by the thorax to a 0.025-cms wide tungsten rod using UV-activated glue (Loctite 3104 Light Cure Adhesive, Loctite, Düsseldorf, Germany). Prior to testing, the tethered mosquitoes were rested upside down in a transparent container lined with moist paper towels to avoid dehydration, and allowed to recover for at least 20 minutes.

Virtual reality flight simulator with acoustic setup

The flight responses of tethered mosquitoes to acoustic and visual stimuli were measured in a flight simulator arena, situated in a dark room maintained at 25±1°C. The simulator's core was a cylindrical LED array featuring a 96×16-pixel grid, with each pixel subtending 3.75° on the mosquito's eye at the azimuth. The flight simulator has been used in *Drosophila* and now mosquito research.[30,74–77] Subjects were secured in a fixed position within the arena at a 45° pitch angle and positioned under an infrared diode. The position of the mosquito was adjusted until the shadow of the beating wings was detectable by an optical wingbeat analyzer situated underneath the subject (Figure 1A). This analyzer converted the shadow's movements into quantifiable data, capturing both the wingbeat amplitude (WBA) and wingbeat frequency (WBF) for analysis.

Challenges arose in measurements from wingbeat analyzer due to the shallow stroke angle of mosquito wings (∼ 40°), yielding extremely noisy data when computing differences in left and right WBA.[30] This contrasts with the larger differences in left and right WBA observed during steering in other species, such as Drosophila, which exhibit stroke angles near 140°.[78] To enhance data accuracy, we supplemented our setup with a Firefly USB 2.0 camera (60 frames/s; Model FMVU-03MTM-CS, Point Grey Research Inc., Richmond, BC, Canada) with an infrared (IR) filter (Midwest Optical System, Inc., Palatine, IL, USA) and employed Kinefly, an open source machine-vision software utilizing an edge detection algorithm to detect wingbeat amplitude.[79] This system enabled more reliable tracking of mosquitoes' WBA in each video frame. However, we observed that some mosquitoes exhibited excessive leg movements, which interfered with the edge detection of wing strokes. Such individuals were excluded from subsequent analysis.

For the delivery of close-range acoustic stimuli, we integrated the audio output from a computer (Dell Optiplex 7080, Dell Technologies, Austin, TX, USA) equipped with a sound card (Audiophile 2496, M-Audio, Cumberland, RI, USA) into the setup. The audio was amplified using a headphone amplifier (DAC-X6, FX-Audio, Shenzhen, China) and delivered to the tethered mosquitoes via one channel of a stereophone (KOSS Corporation, Milwaukee, WI, USA) positioned directly in front of the subject above the LED panels (Figures 2A and S1). Acoustic cues were presented from the front because sounds traveling along the horizontal plane are effective at being detected by mosquitoes than sounds traveling in the vertical plane.[80] To verify that the sounds were playing during audio stimulus delivery, the unused stereophone channel was placed outside the simulation arena along with a calibrated particle velocity microphone (Knowles NR-23158, Itasca, IL, USA) coupled to an audio interface (M2 interface, MOTU, Cambridge, MA, USA) for digitizing sound input. All data, including the sound stimulus from the stereophone, wingbeat amplitude from the camera, and wingbeat frequency from the wingbeat analyzer, were recorded at a sampling rate of 2000 Hz, which exceeds the Nyquist frequency for the male wingbeat frequency. Data acquisition was facilitated by a National Instrument Acquisition board (BNC 2090A, National Instruments, Austin, Texas, USA) and captured using WinEDR v4.0.0 software (University of Strathclyde, Glasgow, UK). The entire flight simulator setup was enclosed in a custom-made sound isolation box (26.5×26.5×28 cm) to prevent sound reflection and interference from external noise. The box was also fitted with a thick acoustic curtain, which was drawn closed during experimental runs for additional sound insulation.

Simulating swarm-like visual scenes on LED panels in the flight simulator

To simulate the visual scenes characteristic *An. coluzzii* swarms, we analyzed fifteen images taken approximately 2 meters from the center of natural swarms. The locations where the images were taken have been sites of previous research on mosquito swarming behaviors in Burkina Faso, West Africa.[8,81,82] These images were processed into binary format, highlighting the mosquitoes as white spots against a black background. We selected a uniform area of 200×200 pixels within regions of high swarm density to determine the percentage of white pixels corresponding to area occupied by mosquitoes. The observed pixel densities varied from 1.6% to 9.1%, averaging at 4.4%. To simulate the visual scenes of swarms on our LED panel, we chose a pixel density of 10%, aligning with the higher end of the natural swarm densities to ensure biological relevance and adequate visual contrast.

Our simulation involved the generation of random starfield patterns on a 96×16 pixel LED panel, using bright pixels set against a dark background to represent the visual contrast in a swarm. This visual environment was also effective at imitating the light intensity characteristic of twilight conditions (0.003 W/m^2 in our setup versus 1-0.0006 W/m^2 from sunset to full lunar illumination).[83] During experimental trials, we presented subjects (both males and females) with wide-field motion of this starfield pattern in open-loop for three seconds, either in clockwise or counter-clockwise direction, and evaluated their tethered flight responses. In a set of preliminary trials, we also tested the response of mosquitoes to wide-field motion of dark pixels on a bright background; however this stimuli failed to elicit a response, suggesting that such visual conditions provided insufficient contrast detection by the mosquitoes.

Moving visual objects with species-specific acoustic cues

To simulate visual aspect of close encounters between mosquitoes within a swarm, we generated square objects in three sizes corresponding to the apparent size of a conspecific at varying distances: 37.5° (10×10 pixels), 22.5° (6×6 pixels), and 15° (4×4 pixels). These sizes were selected to align with or exceed the known visual resolution limits of these mosquitoes[28] and approximate the sight of a neighbor at 1.3, 2.4, and 3.7 body lengths, respectively. Set against a background of the previously described starfield pattern, the brightly pixelated objects were designed to be visually detectable against the contrasting dark environment.

To complement these visual cues with the acoustic cue of nearby flying conspecific, we generated pure tones mimicking the fundamental wingbeat frequency of a female and a male *An. coluzzii*. Such pure tones have been found to be effective at eliciting natural, acoustically guided behaviors in mosquitoes.[80,84] We generated our synthetic in MATLAB and presented at a particle velocity of about 0.04 mm/s, which is about the sound intensity generated by this species at a distance of 2 cm.[54] We did not vary the sound intensity when presenting objects of different sizes to ensure that any observed change in response could be attributed only to object

size. Although this approach may have introduced a minor mismatch between the simulated mosquito's position based on visual and acoustic cues, the different object sizes (0.78 to 2.22 cm) and acoustic stimulus at 2 cm minimize potential mismatches between the visual and acoustic presentations, given that there is an inter-individual variation in flight tone intensity among mosquitoes.[54]

Different group of subjects were assigned to be tested with one of the three object sizes. Multiple open-loop trials were conducted to assess their response to the moving visual object both in isolation and coupled with the male or female flight tones. Prior to the trial's onset, a stationary object within the static starfield background was displayed for two seconds. The trial started with the object's horizontal movement from the left to the right or right to the left visual field, completing two rotations in 6 sec. At the trial's conclusion, the object was held static for an additional two seconds, allowing subjects to return to their baseline flying patterns. The objects moved at an angular velocity of approximately 80°/sec. During acoustic playback trials, the movement of the visual stimulus was synchronized with a six-second flight tone that matched either the male or female flight tones (700 Hz and 450 Hz, respectively). To ensure that any observed changes in tethered flight behavior were due to moving visual objects, most subjects were also tested in control trials with and without acoustic cues where the visual stimulus was solely the static starfield background. Each subject was presented with these varied trials four times in a pseudorandom order to mitigate any potential order effects. The initiation of each trial type was uniquely coded to ensure precise identification during analysis.

Tethered flight data processing

Raw data was analyzed using a custom script in MATLAB R 2023a. First, data were down sampled to 50 Hz to align with the camera's limited frame rate. We then computed additional metrics of differential wingbeat amplitude (L-R WBA) and total wingbeat amplitude (L+R WBA) at each frame using the recorded left and right wingbeat amplitudes. For each trial, baseline measurements of L-R WBA, L+R WBA and wingbeat frequency (WBF) were determined by averaging the values over a one-sec window preceding the start of the trial. Normalized responses for each trial were calculated by subtracting this baseline from the responses recorded during the entire trial period.

Trials where mosquitoes ceased to fly – evidenced by a wingbeat frequency drop below 350 Hz – or exhibited spurious data, as indicated by weak correlation in wingbeat patterns between the left and the right wings (< 0.6), were excluded from analysis. To standardize the data, responses to stimuli moving from right to left were adjusted to reflect responses to left to right motion. The mean normalized response across time was then calculated for each treatment (rotating starfield or moving visual object, moving visual object+female sound, moving visual object+male sound) and control group (static starfield, static starfield+female sound, static starfield+male sound) by averaging responses across replicated trials.

For each treatment group per object size, we collected responses from a minimum of 45 subjects. In total, individual responses from 193 male and 95 female *An. coluzzi* has been used for this study.

Free-flight data processing

We obtained a dataset from[44] comprised of six swarming events of male *An. coluzzii* mosquitoes, which provided us with 938 trajectories for analysis. The dataset captured the motion of each mosquito in a swarms of 13-27 individuals at a sampling rate of 50Hz in laboratory conditions, providing information on their three-dimensional locations over time. Additionally, we had at our disposal calculated velocity and acceleration vectors for each recorded frame. We analyzed this information using MATLAB R 2023a.

For each mosquito within the swarm, we identified its nearest neighbor at each frame and calculated flight parameters, such as acceleration towards nearest neighbor as well as magnitude of acceleration, speed, angular velocity, and flight direction relative to the position of the nearest neighbor. The acceleration towards nearest neighbor was determined by projecting the mosquito's instantaneous acceleration onto the unit vector towards its nearest neighbor. This measurement allowed us to infer the effective inter-individual forces, with positive values indicating attraction and negative values suggesting repulsion. Flight direction relative to the nearest neighbor was quantified by the angle between the mosquito's velocity vector and the unit vector towards its nearest neighbor. Angular measures of 0°, 90° and 180° correspond to the mosquito flying directly towards, perpendicular to, and directly away from its neighbor, respectively.

To determine whether the observed flight dynamics were influenced by the presence of proximal neighbors or were a result of the general swarming motion, we implemented a time-shift analysis. In this analysis, each mosquito's position at time t was virtually transplanted to the same position at time t+1 sec within the swarm. This transplantation allowed us to measure flight parameters of the same mosquito at t relative to its 'virtual' nearest neighbor at t+1sec and thus, compare the flight dynamics of mosquitoes in the presence of actual neighbors against those with the introduced 'virtual neighbors' in control scenarios. For this time-shifted analysis, we evaluated various time-shifted intervals beyond the initial 1-sec shift, and across different intervals, we consistently observed similar trends in the flight dynamics.

QUANTIFICATION AND STATISTICAL ANALYSIS

All statistical analyses were conducted using the R software, version 4.3.1. Across all analyses, *P-values* for pairwise treatment comparisons were adjusted using the Holm method and a significant criterion of 0.05 was used for all statistical testing.

Response to rotating starfield patterns

To discern the influence of rotating starfield patterns on tethered mosquito behavior, we applied pairwise t-tests. These tests compared the subjects' normalized steering responses (L-R WBA) and wingbeat kinematics (L+R WBA and WBFs) during the last second of rotating stimulus presentation against baseline responses recorded in the one-sec interval preceding the stimulus onset. We focused on the last second of stimulus presentation to account for the delay in responses. However, our results were consistent across various time intervals after accounting for the response delay.

Before performing the t-tests, we evaluated the normality of our data distributions by visualizing probability density curves for each variable. Our analysis indicated that all distributions, except one, approximated normality. In the case where normality was questioned due to evident deviation, we conducted a non-parametric Wilcoxon signed-rank test to verify our results. The outcome from the Wilcoxon test was congruent with that obtained from the t-test, reinforcing the reliability of our findings despite the violation to normality assumption in that specific instance.

Response to moving objects

When analyzing the visual response to a small moving object, we restricted our consideration to the initial 3 seconds of stimulus presentation, during which the object completed one turn across the visual field. This decision was informed by an observed perturbation point occurring at 3 seconds, where the object's location reset, causing it to appear in the opposite visual field. This perturbation introduced variability in baseline responses, complicating the interpretation and analysis for the latter half of the stimulus duration. Responses to the full 6-sec stimulus are presented in the supplemental information.

To examine steering responses in these trials, paired t-tests were again used to evaluate changes in steering behavior by contrasting the last second of the stimulus cycle with the one second of pre-stimulus baseline. Although peak steering responses did not uniformly occur within the last second of stimulus cycle, results were consistent across various stimulus intervals after the initial 1.5 sec. Given the large sample size ($N > 45$) across each treatment condition, t-tests were deemed suitable for statistical testing according to the central limit theorem.[85] Nonetheless, we also conducted Wilcoxon signed-rank tests to verify robustness against potential deviations from normality (refer to Table S8). The statistical outcomes from these non-parametric tests aligned perfectly with those from the t-tests, reinforcing our conclusions. Additionally, Spearman's correlation analyses were performed to examine the relationship between the average responses and the object's location during the 0.75 to 2.25-sec window (gray regions in Figures 2 and 3), when the responses appeared to vary monotonically with the object's location.

Since aerodynamic thrust, measured through L+R WBA and WBF, appeared to modulate in relation to the object's location, we performed two Spearman's correlations assessing wing kinematics while the object was moving in front of the mosquito's visual field (0-1.5 sec) and to when it was moving away (1.5-3 sec). Subsequently, pairwise t-tests were then applied to determine whether the thrust responses during these distinct time frames, were statistically distinguishable. Robustness of our statistical results were again confirmed through additional non-parametric Wilcoxon tests. For L+R WBA, results were entirely consistent with those from t-tests (Table S9). For WBF, the Wilcoxon tests revealed differences in statistical outcomes for three treatments (highlighted in Table S10; Figure 4C), although these did not impact the conclusions of the experiment.

Finally, to assess whether changes in flight responses compared to the baseline, denoted by Δ L-R WBA, ΔL+R WBA, and ΔWBF, were dependent on acoustic treatments and object sizes, we fitted linear mixed-effect models (LMMs) to account for repeated measurements. We fitted two nested LMMs for each of the three response variables. The first model included the fixed effects of acoustic treatments, object size as predictor variables and the random effect of subject ID. The second model included an additional interaction term of acoustic treatments $\times$ object size. ANOVAs were used to compare these nested models and thus, test if the interaction term was significant. The first model without the interaction term was adopted if no significant differences were found. For each model, we assessed the residuals for linearity, normality, and homogeneity of variance. Linear mixed effects models are generally robust to normality violations, except in the cases of bimodal distribution.[86] Therefore, the models were accepted even if there were minor deviations from normality.

Free-flight analysis

To investigate the impact of proximity to a neighbor on flight dynamics, we stratified nearest-neighbor distances into discrete categories of 2 cm scale: distances under 2 cm formed one group, distances between 2 cm and 4 cm composed another group, and so forth. For each calculated flight parameter, we fitted a LMM model. This model included categorized distances, treatment conditions (real swarm versus the control with virtual neighbors) and their interaction as fixed effects. Using the fitted model, we compared the flight parameters between real swarm and control conditions across varying distances.

Given the longitudinal nature of our data, where flight parameters of each mosquito within a swarm were measured over time, we initially attempted to incorporate a nested random effect structure in our model. This structure was intended to account for repeated measures of individual mosquitoes within swarms, with time as a random slope to adjust for temporal variations in flight activity. However, this approach violated the assumption of homogeneity in variance due to complex random structure. Consequently, we simplified the random effects structure to account for repeated measures from the same swarms. In some cases, we also had to log transform the flight parameter to satisfy the model assumptions.